RSC Advances

PAPER

View Article Online
View Journal | View Issue

Cite this: *RSC Adv.*, 2021, **11**, 5156

Silky Co_3O_4 nanostructures for the selective and sensitive enzyme free sensing of uric acid

Abdul Sattar Chang,[a] Aneela Tahira,[a] Fouzia Chang,[a] Nusrat Naeem Memon,[a] Ayman Nafady,[b] Amal Kasry[c] and Zafar Hussain Ibupoto *[a]

In this study, simple, new and functional silky nanostructures of Co_3O_4 are prepared by hydrothermal method. These nanostructures are successfully used for the enzyme free sensing of uric acid in 0.1 M phosphate buffer solution of pH 7.3. Physical characterization experiments were carried out to explore the morphology, composition and crystalline phase of the newly prepared Co_3O_4 nanostructures. Scanning electron microscopy (SEM) shows a silk like morphology and energy dispersive spectroscopy (EDS) revealed the presence of Co and O as the main elements. Powder X-ray diffraction (XRD) demonstrates a cubic crystallography with well resolved diffraction patterns. The electrochemical activity of these silky Co_3O_4 nanostructures was evaluated by cyclic voltammetry (CV) in a 0.1 M phosphate buffer solution at pH 7.3. The high purity and unique morphology of Co_3O_4 shows a highly sensitive and selective response towards the non-enzymatic sensing of uric acid. This uric acid sensor exhibits a linear range of 0.5 mM to 3.5 mM uric acid and a 0.1 mM limit of detection. The anti-interference capability of this uric acid sensor was monitored in the presence of common interfering species. Furthermore, electrochemical impedance spectroscopy confirms a low charge transfer resistance value of 5.11 K Ω cm^2 for silky Co_3O_4 nanostructures which significantly supported the CV results. The proposed modified electrode is stable, selective and reproducible which confirms its possible practical use. Silky Co_3O_4 nanostructures can be of great importance for diverse electrochemical applications due to their excellent electrochemical activity and large surface area.

Received 12th December 2020
Accepted 22nd January 2021

DOI: 10.1039/d0ra10462k

rsc.li/rsc-advances

1. Introduction

Uric acid (UA) is an important biological molecule present in the blood and urine. UA is an antioxidant which is a final product of purine metabolism in the human body.[1,2] The normal physiological level of UA in the human blood is 0.13 to 0.46 mM.[3] However, a high level of UA in the blood serum leads to several pathological diseases such as hyper-uricemia, gout, pneumonia,[4] chronic nephritis, chronic pneumonia, podagra, cancer, hyperuricemia arthritis, and nephropathy.[5] Abnormal level of UA in the blood causes kidney disease, obesity, high blood pressure *etc.*[6–8]. Many studies have suggested that the high level of UA in serum is also a risk factor for heart diseases.[9] Due to the significant importance of these pathologies, it is very important to develop an effective analytical methodology for the accurate measurement of UA. So far, different analytical methods such as high performance liquid chromatography,[10] fluorescence spectroscopy,[11] colorimetry,[12] capillary electrophoresis,[13] chemiluminescence[14] *etc.* have been used for the determination of UA. These techniques are expensive, complicated, time consuming, involve sophisticated tools that make them unsuitable for the quantitative determination of UA. In order to overcome these problems, electrochemical techniques have received significant interest for the detection of analytes because of their simplicity, low cost, rapid response and high sensitivity.[15–20] Due to high electroactive nature of UA, its determination by electrochemical methods has been established.[21–25] Electrochemical determination of UA is carried out by both enzymatic[26] and non-enzymatic[17] approaches. Enzyme based UA biosensors use uricase as an enzyme for the oxidation of uric acid.[26] There are so many drawbacks associated with enzyme based electrochemical biosensors like complicated immobilization of enzymes, lack of reproducibility, high cost and their environment dependent activity.[27] Non-enzymatic approach involves the oxidation of UA on the surface of suitable electrode[17] material. Various electrochemical modes such as cyclic voltammetry,[26] amperometry,[28–31] differential pulse voltammetry (DPV),[17] square wave voltammetry[32] *etc.* have been used for the sensing of UA from different samples. To prepare a potential catalytic active material is the main requirement for the enzyme free sensing of uric acid, but it is still a big challenge. In last few decades, transition metal oxides such as

[a]*Dr. M.A Kazi Institute of Chemistry, University of Sindh, Jamshoro, 76080, Sindh, Pakistan. E-mail: zaffar.ibhupoto@usindh.edu.pk*

[b]*Department of Chemistry, College of Science, King Saud University, Riyadh 11451, Saudi Arabia*

[c]*Nanotechnology Research Centre (NTRC), The British University in Egypt (BUE), Egypt*

Co_3O_4, ZnO, Fe_3O_4, MnO_2, and NiO show attractive applications in electrochemical sensing.[33–37] Among them, cobalt oxide (Co_3O_4) is best choice because of its special properties such as low cost, non-toxic, and excellent chemical durability *etc.*[38] Moreover, Co_3O_4 is composed of mixed Co^{2+} and Co^{3+} ions located on tetrahedral and octahedral site respectively which play a significant role in the electrochemical activity of Co_3O_4.[39] Furtherer more, Co_3O_4 material has been hybridized with different materials such as graphene, graphene oxide, quantum dots, carbon nanotube to improve the electron transfer tendency of Co_3O_4 modified electrode.[40–42] Also, Co_3O_4-based nanocomposites have been reported in the literature for the electrochemical determination of UA.[39,43] Despite the superior performance of composite materials, however they involve complicated steps during their synthesis and require highly sensitive analytical techniques to characterize them. Therefore, both high cost during the synthesis and characterization again allow the researchers to think and design new pristine materials with outperform functionalities. For this purpose, we used an equal volume ratio of organic (ethylene glycol) and inorganic (water) as a solvent for the growth of Co_3O_4 by hydrothermal method and we obtained a silky morphology with an excellent electrochemical activity. The synthetic strategy is simple and low cost, thus it can be considered as the front line for the mass production of functional Co_3O_4 materials. In this study, we have prepared a silky morphology of Co_3O_4 by hydrothermal method using equal volumes of organic and inorganic solvents. The SEM, EDS and XRD have well characterized the physical features of Co_3O_4. These silky nanostructures of Co_3O_4 were used for the enzyme free sensing of uric acid and sensor exhibits a linear range of 0.5 mM to 3.5 mM uric acid and a 0.1 mM limit of detection. The newly developed uric acid sensor is also highly selective and stable.

2. Materials and methods

2.1 Chemical reagents

All the chemicals like cobalt chloride hexahydrate (99%), urea (99%), ethylene glycol (60%), uric acid (99%), glucose (99%), lactic acid (85%), sodium chloride (99%), potassium chloride (99%) and 5% Nafion (E.W. 1100) were of analytical grades and used as received without any further purification. These chemicals were supplied by the Sigma Aldrich Karachi Pakistan. All the solutions were prepared in the deionized water having a resistivity of 18.2 (megohm). An electrolyte of 0.1 M phosphate buffer solution of pH 7.3 was prepared by mixing potassium dihydrogen phosphate (KH_2PO_4) (0.1 M) (99%), sodium hydrogen phosphate (Na_2HPO_4) (0.1 M) (99%), and sodium chloride (NaCl) (0.135 M) (99%). The pH of buffer solution was maintained by adding 0.1 M NaOH (99%) and HCl (37%).

2.2 Synthesis of silky Co_3O_4 nanostructures

Hydrothermal method was used to prepare silky Co_3O_4 nanostructures. The precursor solution of 0.1 M cobalt chloride hexahydrate and 0.1 M urea was prepared in the equal volume of organic (ethylene glycol) and inorganic (water) solvents with volume ratio of 1 : 1. Then reaction for the synthesis of Co_3O_4 was carried out under hydrothermal conditions at 150 °C for 12 h in stainless autoclave. Then the autoclave was naturally cooled at room temperature and nanostructured product was obtained on the ordinary filter paper. After the drying of metal hydroxide material for overnight then a thermal annealing was carried out in the crucible at 500 °C in air for 4 h in muffle furnace to obtain the Co_3O_4 nanostructures. The structural, compositional and crystallographic studies were carried out at low resolution SEM, EDS and powder XRD analytical techniques respectively. The SEM and EDS measurements were performed using a field emission scanning electron microscope (Quattro S from Thermo Fisher) at an accelerating voltage of 20 kV. The powder XRD measurement was done at CuKα radiation (λ = 1.5418 Å), 45 kV and 45 mA.

2.3 Electrochemical sensing of uric acid using silky Co_3O_4 nanostructures

The prepared Co_3O_4 sample (8 mg) was dispersed in 2.5 mL of de-ionized water and 0.5 mL of Nafion (5%) and sonicated for the 25 minutes to ensure the proper dispersion of nanomaterial. Before modification, bare glassy carbon electrode (BGCE) was polished with alumina paste and cleaned with ethanol and water for 2 minutes respectively. After that, glassy carbon electrode was modified with approximately 10 μL of prepared Co_3O_4 by drop casting method. A three electrode system was used in which Ag/AgCl (saturated with 3 M KCl) acts as a reference electrode, modified glassy carbon electrode (MGCE) with Co_3O_4 as working electrode and platinum wire was used as a counter electrode. All the electrochemical measurements were performed by cyclic voltammetry in the potential window of −0.4 V to 8.0 V at a scan rate of 50 mV s^{-1} except scan rate study. Electrochemical impedance spectroscopy study carried out at frequency range from 100 kHz to 1 Hz, sinusoidal potential of 5 mV and biasing potential of 0.35 V in 1 mM uric acid solution. A 0.1 M phosphate buffer solution of pH 7.3 was used as electrolyte and 5 mM stock solution of uric acid was prepared in it. The low concentrate solutions of uric acid were prepared in the phosphate buffer solution and all electrochemical experiments were performed at room temperature.

3. Results and discussion

3.1 Morphology and crystalline structure studies of newly prepared Co_3O_4 nanostructures

The distinctive morphology of as prepared Co_3O_4 nanostructures in the organic and inorganic solvent media was investigated by scanning electron microscopy as shown in Fig. 1. Fig. 1(a and b) shows the typical SEM image at low and high magnifications and it can be seen that the Co_3O_4 material exhibits a silky morphology. The thickness of silky sheets is few nm and they also have large surface area which can easily allow the uric acid molecule to adsorb and oxidize efficiently. The chemical elements like Co and O were identified by EDS indicating the high purity of as prepared Co_3O_4 material as shown in Fig. 1(c). Furthermore, to understand the chemical

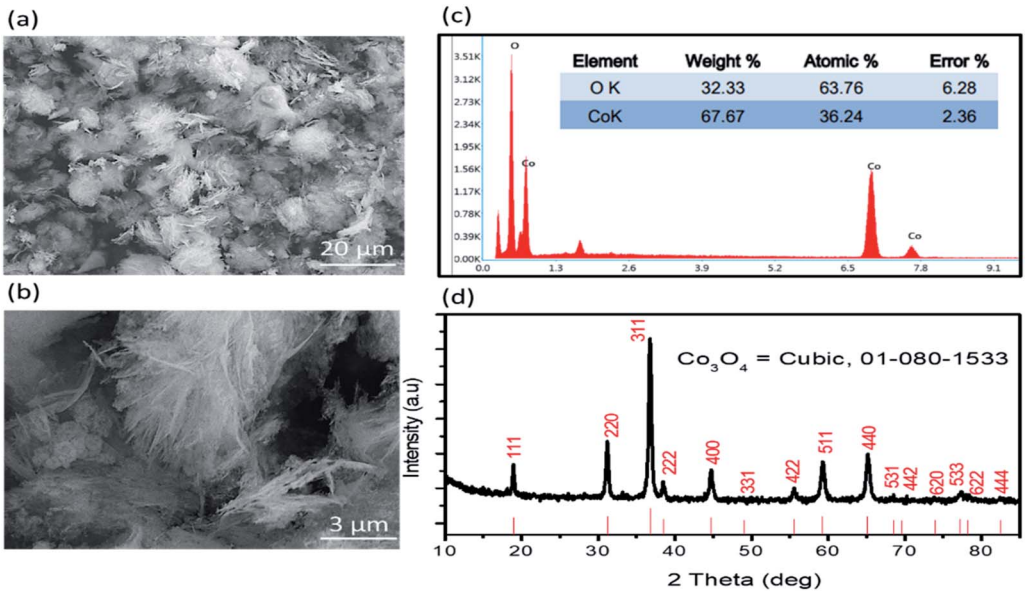

Fig. 1 (a and b) Typical SEM images of Co_3O_4 at different magnifications, (c) EDS spectrum of Co_3O_4, (d) powder XRD diffraction patterns of Co_3O_4.

composition and crystallography of Co_3O_4 nanostructures, powder XRD was used to measure the diffraction patterns as enclosed in Fig. 1(d). The diffraction patterns are well resolved and supported by the reference (card no: 01-080-1533). The XRD study confirms the cubic phase of Co_3O_4 and its high purity. The chemical composition results of Co_3O_4 by XRD and ED's analysis are in good agreement.

3.2 Electrochemical sensing toward oxidation of uric acid using silky Co_3O_4 nanostructures

Cyclic voltammetry was used to explore the electrochemical activity of silky Co_3O_4 nanostructures in 0.1 M phosphate buffer solution of pH 7.3. Fig. 2 shows the cyclic voltammogram of bare glassy carbon electrode (BGCE) in the electrolyte aqueous solution and uric acid, and Co_3O_4 modified glassy carbon electrode (MGCE) in the presence of aqueous solution of uric acid and electrolyte. The Co_3O_4 MGCE has shown the well-shaped oxidation peak for the uric acid at 0.35 V in 1 mM uric acid. The BGCE has shown no electrochemical activity for the uric acid. These improved electrochemical activity results of silky Co_3O_4 are attributed due to fascinating morphology of Co_3O_4 which could be compatible with the uric acid molecules towards the catalytic oxidation. The working principle of enzyme free uric acid sensor based on the nanostructured materials is not well described in the literature, however we propose it on the basis of molecular structure of uric acid which involves the two electron and two proton transfer process[44,45] as shown in Scheme 1. The silky features of Co_3O_4 are providing the large surface area and exposure of abundant catalytic sites for the oxidation of uric acid. Another, the possible reason for the enzyme free detection on the surface of Co_3O_4 could be its p-type (excess of hole concentration) semiconducting features which facilitated the easily capture of electrons from the oxidation of uric acid. From CV curve as shown in Fig. 2, an irreversible and highly resolved peak at 0.35 V was noticed with the use of silky Co_3O_4 nanostructures. It suggests the swift electron transfer kinetics by the silky Co_3O_4 nanostructures with enhanced the oxidation peak current and high density of catalytic sites for the uric acid oxidation. Further to add, the uric acid follows the Nernst equation which suggests that the oxidation of uric acid is governed by the two proton and two electron transfer as enclosed in the Scheme 1. This leads to instability of uric acid and possible formation of uric acid derivatives.[46] The presence of silky Co_3O_4 nanostructures might enhance the density of catalytic sites on its surface. The uric acid and its derivatives, enable the variation in the electron transfer and a rise in the oxidation peak current is significant.[47,48]

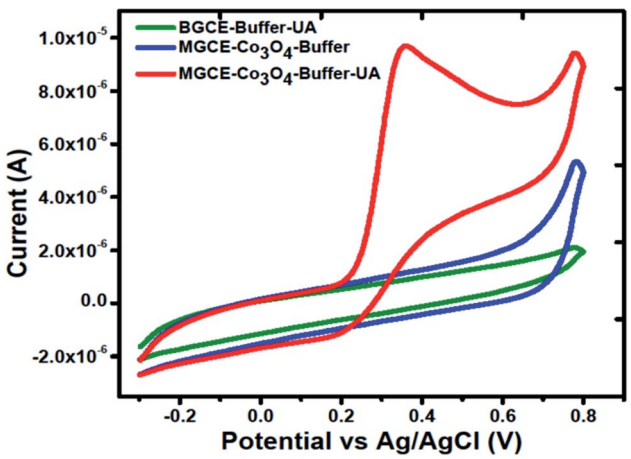

Fig. 2 Cyclic voltammogram of MGCE with Co_3O_4 in the 0.1 M phosphate buffer solution of pH 7.3, and BGCE and MGCE with Co_3O_4 in the presence of 1 mM uric acid at a scan rate of 50 mV s^{-1}.

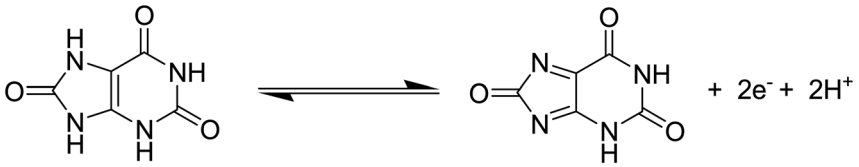

Scheme 1 The oxidation mechanism of uric acid.

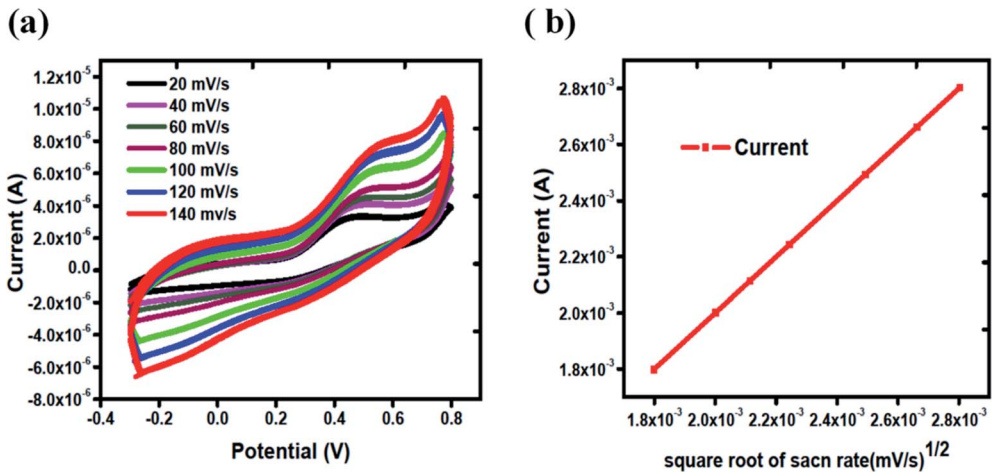

Fig. 3 (a) Cyclic voltammograms of Co_3O_4 from 20 mV s^{-1} to 140 mV s^{-1} in 1 mM uric acid, (b) linear fit of oxidation peak current *versus* square root of scan rates.

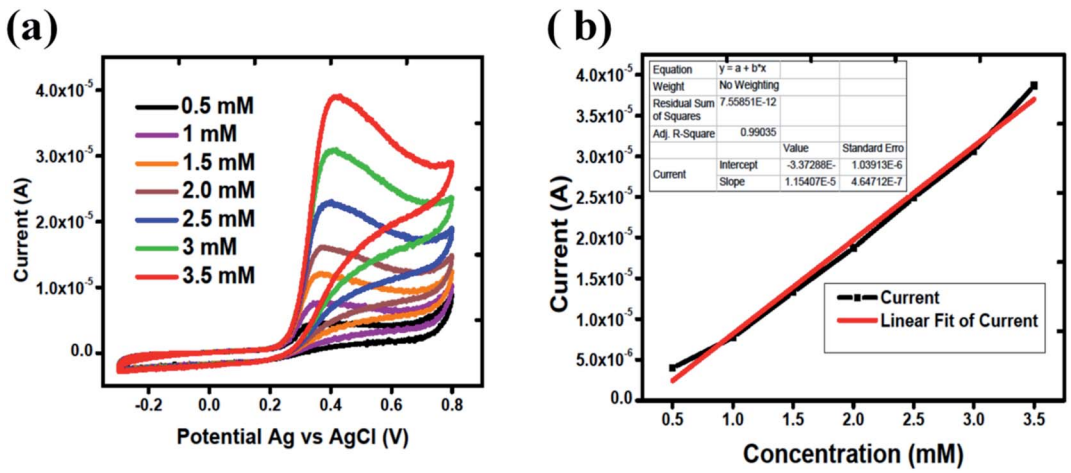

Fig. 4 (a) Cyclic voltammograms of Co_3O_4 for different 0.5 mM to 3.5 mM uric acid concentrations at a scan rate of 50 mV s^{-1}, (b) linear fitting of oxidation peak current *versus* various uric acid concentrations.

The electrode kinetics towards the oxidation of uric acid was explored at different scan rates. Fig. 3(a) shows the scan rate study of Co_3O_4 from 20 mV s^{-1} to 140 mV s^{-1} in 1 mM uric acid. It is obvious that the oxidation peak current was increased linearly with increasing value of scan rate. Fig. 3(b) shows the linear fit of the peak current *versus* square root of the scan rate. The linear plot between the peak current and square root of scan rate suggests the kinetically controlled chemical reaction on the surface of MGCE using silky nanostructures of Co_3O_4.

The linear range of proposed uric acid sensor was obtained at different concentrations of uric acid in phosphate buffer solution of pH of 7.3. Fig. 4(a) shows the calibration study of Co_3O_4 in the range of 0.5 mM to 3.5 mM of uric acid. Cyclic voltammograms show that there is regular increase in the oxidation peak current with the increasing concentration of uric acid which indicates an excellent quantitative response of the proposed Co_3O_4 material for the determination of uric acid. Fig. 4(b) indicates the linear fitting of oxidation peak current

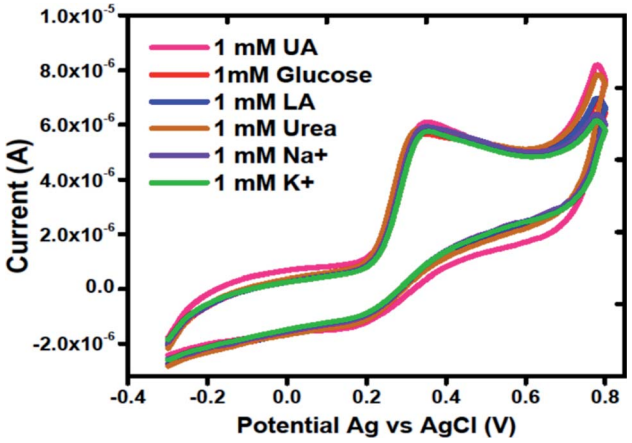

Fig. 5 Cyclic voltammogram curves at a scan rate of 50 mV s^{-1} of different interfering substances using silky nanostructures of Co_3O_4 in 1 mM uric acid.

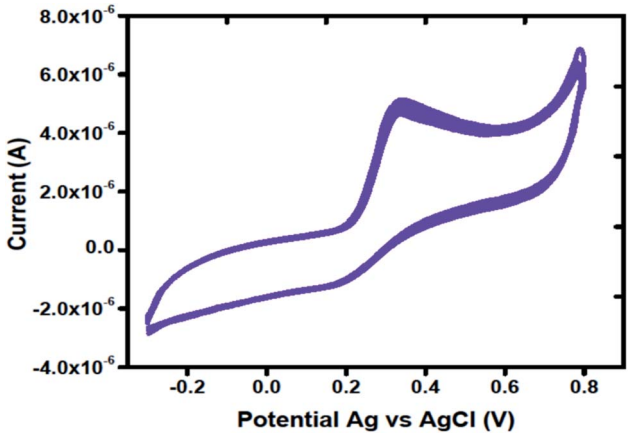

Fig. 6 Cyclic voltammetry curves at a scan rate of 50 mV s^{-1} for measuring the stability of Co_3O_4 in the presence of 1 mM uric acid.

versus various uric acid concentrations with regression coefficient of 0.99. The limit of detection was measured according to the reported work.[49] The limit of detection of silky Co_3O_4 nanostructures was found to be 0.1 mM.

It is notable that the selectivity is significant parameter in the evaluation of performance of electrochemical method. Various electrochemically active substances present in the biological samples may interfere during the determination of uric acid. For this reason, interference study of Co_3O_4 was carried out in the presence and absence of possible interfering substances such as glucose, lactic acid, urea, sodium ions and potassium ions using same concentration of each of them. Fig. 5 shows the cyclic voltammogram of MGCE with Co_3O_4 in 1 mM uric acid. Different interfering substances slightly lead to a maximum of 5% change in the current intensity. Hence, the sensor showed a good selectivity towards the detection of uric acid.

The stability of MGCE with Co_3O_4 was checked through several CV curves in 1 mM of uric acid. Fig. 6 shows the CV

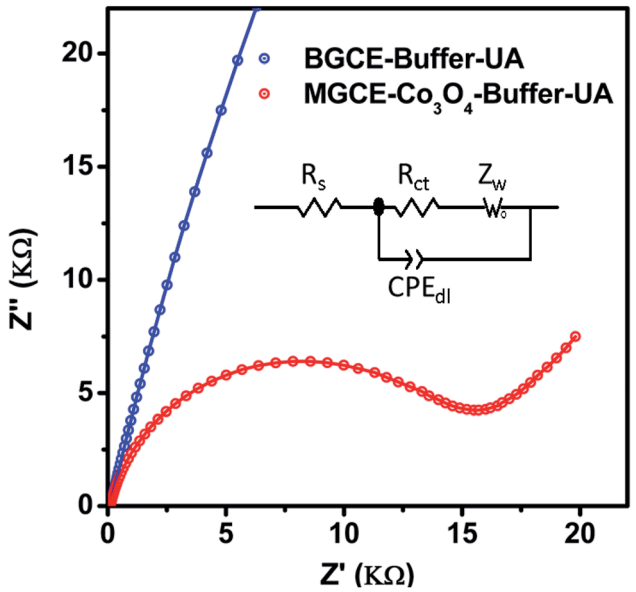

Fig. 7 Nyquist plots of BGCE and MGCE with Co_3O_4 material in 1 mM uric acid solution, inset shows the equivalent circuit model with circuit elements.

curves after 15 successive runs at a scan rate of 50 mV s^{-1}. The CV curves shown in Fig. 6 clearly demonstrates the excellent stability of proposed Co_3O_4 material; thus it can be used for the determination of uric acid without a signal drop.

Further to validate the CV results enclosed in Fig. 2, an electrochemical impedance spectroscopy was performed to get a deep sight about the electron transfer kinetics of BGCE and MGCE with Co_3O_4. Fig. 7 shows the Nyquist plots of BGCE and MGCE and inset is indicating the fitted equivalent circuit model with circuit elements such as solution resistance (R_s), charge transfer resistance (R_{ct}), Warburg diffusion element (Z_w), and constant phase elements (CPE). The charge transfer resistance values were estimated from the simulated data by zview software. The calculated charge transfer resistance values were obtained 385.88 K Ω cm^2 and 15.11 K Ω cm^2 for BGCE and MGCE with Co_3O_4 respectively. The low charge transfer resistance of MGCE compared to BGCE has revealed the superior conductivity of Co_3O_4 and improved electrochemical properties and these obtained results have strongly supported the CV results.

The performance of proposed uric acid sensor was compared with the reported works as given in Table 1. It is obvious that, the prepared Co_3O_4 material has shown a superior or equal electrochemical activity in the wide range from 500 μM to 3500 μM of uric acid concentrations as compared to the previous works. There is no report on the silky Co_3O_4 material which gives of electrochemical signal above 600 μM of uric acid. The limit of detection is bit high, but still in the range of physiological conditions. Hence the proposed silky nanostructures of Co_3O_4 may be used for the determination of uric acid at higher concentrations.

Table 1 The comparison of performance of proposed enzyme free uric acid sensor with reported works

Modified electrodes	Electrochemical mode	Linear range, μM	LOD, μM	Reference
PCN[a]/MWCNT[b]	CV and DPV	0.2–20 μM	0.139 μM	44
B-MWCNTS[c]	CV, EIS[d]	62–250 μM	0.65 μM	45
Pd/RGO[e]	CV, DPV	6–469.5 μM	1.6 μM	17
Au/RGO[e]	CV	8.8–53 μM	1.8 μM	2
PtNi@MoS_2[f]	CV, DPV	0.5–600 μM	0.1 μM	50
Cysteic acid	DPV	1.0–19 μM	0.36 μM	51
Co_3O_4	CV	500–3500 μM	100 μM	Current work

[a] Porous g-C_3N_4. [b] Multi-walled carbon nanotubes. [c] Boron-doped multiwalled carbon nanotubes. [d] Electrochemical impedance spectroscopy. [e] Reduced graphene oxide. [f] PtNi bimetallic nanoparticles loaded MoS_2 nanosheets.

4. Conclusions

In summary, we have prepared new silky nanostructures of Co_3O_4 by hydrothermal method under the equal volume of organic and inorganic solvents. The physical characterization has shown a silk like morphology and cubic crystallography. The chemical composition of Co_3O_4 was mainly governed by the presence of Co and O elements. The electrochemical activity of Co_3O_4 material was studied in 0.1 M phosphate buffer solution of pH 7.3 for the determination of uric acid. The silky Co_3O_4 nanostructures exhibited an excellent catalytic activity due to large surface area which easily allow the uric acid molecules to oxidize successfully. The enzyme free sensor based on silky Co_3O_4 nanostructures possessed a linear range from 0.5 mM to 3.5 mM of uric acid. The limit of detection was estimated around 0.1 mM. The modified electrode is highly selective and stable. The obtained results from CV and the electrochemical impedance spectroscopy are in good agreement. Based on the electrochemical activity, we are confident that the silky Co_3O_4 nanostructures could be of great worth to be investigated in the wide range of electrochemical applications.

Conflicts of interest

Authors declare no conflict of interest in this research work.

Acknowledgements

The authors thank the British University in Egypt for the support in the SEM imaging through the Nanotechnology Research Centre. A. N. thanks Researchers Supporting Project number (RSP-2021/79) at King Saud University, Riyadh, Saudi Arabia.

References

1 M. Mohamadi, A. Mostafavi and M. Torkzadeh-Mahani, *Biosens. Bioelectron.*, 2014, **54**, 211–216.
2 C. Wang, J. Du, H. Wang, C. e. Zou, F. Jiang, P. Yang and Y. Du, *Sens. Actuators, B*, 2014, **204**, 302–309.
3 L. Rana, R. Gupta, M. Tomar and V. Gupta, *Sens. Actuators, B*, 2018, **261**, 169–177.
4 B. F. Culleton, M. G. Larson, W. B. Kannel and D. Levy, *Ann. Intern. Med.*, 1999, **131**, 7–13.
5 A. G. Sarıkaya, B. Osman, T. Çam and A. Denizli, *Sens. Actuators, B*, 2017, **251**, 763–772.
6 E. Liberopoulos, D. Christides and M. Elisaf, *J. Hypertens.*, 2002, **20**, 347.
7 F. Mateos and J. Puig, *J. Inherited Metab. Dis.*, 1994, **17**, 138–142.
8 R. J. Johnson, D.-H. Kang, D. Feig, S. Kivlighn, J. Kanellis, S. Watanabe, K. R. Tuttle, B. Rodriguez-Iturbe, J. Herrera-Acosta and M. Mazzali, *Hypertension*, 2003, **41**, 1183–1190.
9 M. Alderman and K. J. Aiyer, *Curr. Med. Res. Opin.*, 2004, **20**, 369–379.
10 N. Cooper, R. Khosravan, C. Erdmann, J. Fiene and J. W. Lee, *J. Chromatogr. B: Anal. Technol. Biomed. Life Sci.*, 2006, **837**, 1–10.
11 X. Lian and B. Yan, *Inorg. Chem.*, 2017, **56**, 6802–6808.
12 X. Chen, J. Chen, F. Wang, X. Xiang, M. Luo, X. Ji and Z. He, *Biosens. Bioelectron.*, 2012, **35**, 363–368.
13 A. Makrlíková, F. Opekar and P. Tůma, *Electrophoresis*, 2015, **36**, 1962–1968.
14 D. Yao, A. G. Vlessidis and N. P. Evmiridis, *Anal. Chim. Acta*, 2003, **478**, 23–30.
15 X. Yang, J. Kirsch and A. Simonian, *J. Microbiol. Methods*, 2013, **95**, 48–56.
16 X. Yang, J. Kirsch, E. V. Olsen, J. W. Fergus and A. L. Simonian, *Sens. Actuators, B*, 2013, **177**, 659–667.
17 J. Wang, B. Yang, J. Zhong, B. Yan, K. Zhang, C. Zhai, Y. Shiraishi, Y. Du and P. Yang, *J. Colloid Interface Sci.*, 2017, **497**, 172–180.
18 R. Sha, S. K. Puttapati, V. V. Srikanth and S. Badhulika, *IEEE Sens. J.*, 2017, **18**, 1844–1848.
19 R. Sha and S. Badhulika, *J. Electroanal. Chem.*, 2018, **816**, 30–37.
20 R. Sha, K. Komori and S. Badhulika, *Electrochim. Acta*, 2017, **233**, 44–51.
21 J. C. Ndamanisha and L. Guo, *Biosens. Bioelectron.*, 2008, **23**, 1680–1685.
22 L. Wu, L. Feng, J. Ren and X. Qu, *Biosens. Bioelectron.*, 2012, **34**, 57–62.
23 S. Wu, T. Wang, Z. Gao, H. Xu, B. Zhou and C. Wang, *Biosens. Bioelectron.*, 2008, **23**, 1776–1780.

24 C. Xiao, X. Chu, Y. Yang, X. Li, X. Zhang and J. Chen, *Biosens. Bioelectron.*, 2011, **26**, 2934–2939.
25 A. Özcan and Y. Şahin, *Biosens. Bioelectron.*, 2010, **25**, 2497–2502.
26 K. Arora, M. Tomar and V. Gupta, *Analyst*, 2014, **139**, 837–849.
27 M. B. Wayu, M. A. Schwarzmann, S. D. Gillespie and M. C. Leopold, *J. Mater. Sci.*, 2017, **52**, 6050–6062.
28 C. Zhao, L. Wan, Q. Wang, S. Liu and K. Jiao, *Anal. Sci.*, 2009, **25**, 1013–1017.
29 M. Bhambi, G. Sumana, B. Malhotra and C. Pundir, *Artif. Cells, Blood Substitutes, Biotechnol.*, 2010, **38**, 178–185.
30 S. Kuwabata, T. Nakaminami, S.-i. Ito and H. Yoneyama, *Sens. Actuators, B*, 1998, **52**, 72–77.
31 T. Hoshi, H. Saiki and J.-i. Anzai, *Talanta*, 2003, **61**, 363–368.
32 N. Baig and A.-N. Kawde, *RSC Adv.*, 2016, **6**, 80756–80765.
33 M. Kassaee, E. Motamedi and M. Majdi, *Chem. Eng. J.*, 2011, **172**, 540–549.
34 S. Muthumariappan and C. Vedhi, *IOSR J. Appl. Chem.*, 2017, **10**, 55–64.
35 R. Thangarasu, V. D. Victor and M. Alagumuthu, *Anal. Bioanal. Electrochem.*, 2019, **11**, 427–447.
36 Z.-G. Liu, X. Chen, J.-H. Liu and X.-J. Huang, *Electrochem. Commun.*, 2013, **30**, 59–62.
37 K. M. Zeinu, H. Hou, B. Liu, X. Yuan, L. Huang, X. Zhu, J. Hu, J. Yang, S. Liang and X. Wu, *J. Mater. Chem. A*, 2016, **4**, 13967–13979.
38 S. Dubey, J. Kumar, A. Kumar and Y. C. Sharma, *Adv. Powder Technol.*, 2018, **29**, 2583–2590.
39 M. Venu, V. Agarwa, S. Venkateswarlu and G. Madhavi, *Int. J. Electrochem. Sci.*, 2018, **13**, 11702–11719.
40 A. E. Vilian, B. Dinesh, M. Rethinasabapathy, S.-K. Hwang, C.-S. Jin, Y. S. Huh and Y.-K. Han, *J. Mater. Chem. A*, 2018, **6**, 14367–14379.
41 H. Wang, R. Li and Z. Li, *Electrochim. Acta*, 2017, **255**, 323–334.
42 B. Çakıroğlu and M. Özacar, *Biosens. Bioelectron.*, 2018, **119**, 34–41.
43 B. Hu, Y. Liu, Z.-W. Wang, Y. Song, M. Wang, Z. Zhang and C.-S. Liu, *Appl. Surf. Sci.*, 2018, **441**, 694–707.
44 J. Lv, C. Li, S. Feng, S.-M. Chen, Y. Ding, C. Chen, Q. Hao, T.-H. Yang and W. Lei, *Ionics*, 2019, **25**, 4437–4445.
45 N. G. Tsierkezos, U. Ritter, Y. N. Thaha, C. Downing, P. Szroeder and P. Scharff, *Microchim. Acta*, 2016, **183**, 35–47.
46 G. Dryhurst, *J. Electrochem. Soc.*, 1972, **119**, 1659–1664.
47 L. Wu, L. Feng, J. Ren and X. Qu, *Biosens. Bioelectron.*, 2012, **34**, 57–62.
48 N. Tukimin, J. Abdullah and Y. Sulaiman, *Sensors*, 2017, **17**, 1539.
49 S. Amin, A. Tahira, A. R. Solangi, R. Mazzaro, Z. H. Ibupoto, A. Fatima and A. Vomiero, *Electroanalysis*, 2020, **32**, 1052–1059.
50 L. Ma, Q. Zhang, C. Wu, Y. Zhang and L. Zeng, *Anal. Chim. Acta*, 2019, **1055**, 17–25.
51 Z. Hassanvand and F. Jalali, *Mater. Sci. Eng. C*, 2019, **98**, 496–502.